

Receding-Horizon Maximum-Likelihood Estimation of Neural-ODE Dynamics and Thresholds from Event Cameras

Kazumune Hashimoto, Kazunobu Serizawa, Masako Kishida

Abstract—Event cameras emit asynchronous brightness-change events where each pixel triggers an event when the last event exceeds a threshold, yielding a history-dependent measurement model. We address online maximum-likelihood identification of continuous-time dynamics from such streams. The latent state follows a Neural ODE and is mapped to predicted log-intensity through a differentiable state-to-image model. We model events with a history-dependent marked point process whose conditional intensity is a smooth surrogate of contrast-threshold triggering, treating the contrast threshold as an unknown parameter. The resulting log-likelihood consists of an event term and a compensator integral. We propose a receding-horizon estimator that performs a few gradient steps per update on a receding horizon window. For streaming evaluation, we store two scalars per pixel (last-event time and estimated log-intensity at that time) and approximate the compensator via Monte Carlo pixel subsampling. Synthetic experiments demonstrate joint recovery of dynamics parameters and the contrast threshold, and characterize accuracy–latency trade-offs with respect to the window length.

Index Terms—Event cameras, Temporal point process, Neural ODE, Receding-horizon estimation.

I. INTRODUCTION

Event cameras [1], including the Dynamic Vision Sensor (DVS) [2] and the DAVIS family [3], report asynchronous brightness-change events with microsecond timestamps, high dynamic range, and low latency. Unlike frame-based sensors, they transmit information only when brightness at each pixel changes sufficiently, thereby emphasizing moving edges and reducing motion blur caused by exposure time integration. These properties make event streams well-suited in high-speed and high-dynamic-range settings, enabling optical flow [4]–[6]; high-frame-rate video reconstruction and frame interpolation [7]–[10]; and ego-motion/SLAM datasets and simulators [11], [12]. Recent work also demonstrates that event cameras can reduce perceptual latency in safety-critical perception pipelines [13].

Many event-based pipelines target a single-shot prediction from a fixed spatiotemporal event representation. In contrast, a broad class of applications requires continuous-time state and dynamics estimates for tracking, prediction, online system identification, and feedback control. In these settings, the information needed for estimation is encoded not only in

the event marks (pixel and polarity) but also in fine event timing. This motivates estimators that (i) respect asynchronous timestamps and (ii) provide a likelihood over the raw event stream, so that dynamics parameters can be fit and adapted online in a principled way.

A common description of event generation is contrast thresholding: a pixel fires when the accumulated change in log-intensity since its previous event reaches a threshold. Because the threshold directly affects event timing, it directly impacts dynamics estimation from timestamps. In practice, the effective threshold is often not known precisely and can depend on sensor settings and operating conditions [14], [15]. Treating the threshold as a fixed *known* constant can therefore introduce bias, especially when the inference relies on fine timing structure.

Beyond threshold uncertainty, event streams pose fundamental modeling challenges. Event times are irregular, observations are discrete marks (pixel location and polarity), and event generation is history-dependent because each pixel resets its reference after it fires. A common workaround is to aggregate events into fixed-rate tensors (for example, voxel grids) and apply standard architectures [4], [7], [16]. Such representations are effective for downstream prediction but discretize time and typically do not define a normalized likelihood over the original timestamps. Complementary model-based approaches incorporate event generation mechanisms for reconstruction and filtering, or optimize surrogate objectives such as contrast maximization and alignment under a motion hypothesis [8], [17]–[19]. However, these approaches are usually not formulated as maximum-likelihood estimation of continuous-time dynamics directly from the raw event stream.

A *likelihood-based* alternative is to model an event stream as a marked temporal point process. This provides a normalized probability model over both event times and marks, and it naturally accommodates irregular timestamps and history dependence. A practical challenge is computational cost. Point-process likelihoods include, in addition to a sum over observed events, a normalization (no-event) term that integrates the predicted event rate over time and sums over the full pixel grid. Evaluating this term can dominate runtime especially for long streams, which is particularly problematic in online estimation settings.

In this paper, we develop an online maximum-likelihood estimator for continuous-time dynamics observed through event-camera streams. Its latent state follows a Neural ODE [20] and is mapped to predicted log-intensity through a differentiable

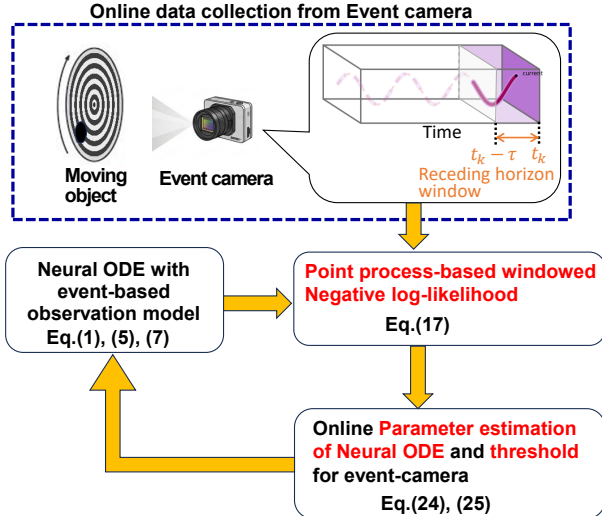


Fig. 1: Illustration of the proposed framework.

state-to-image model. Events are modeled with a history-dependent marked point process whose conditional intensity is a smooth surrogate of contrast-threshold triggering. We treat the pixel-dependent contrast thresholds as unknown parameters and estimate them jointly with the dynamics. To support streaming operation, we maintain a compact per-pixel memory that summarizes the information needed to evaluate history-dependent residuals. We use a fixed-lag receding-horizon scheme that replays only recent events aiming to keep per-update computation bounded.

The contributions of this paper are twofold:

- We introduce a differentiable residual-to-rate mapping as a smooth surrogate of contrast-threshold triggering within a *marked point-process likelihood*, enabling joint estimation of dynamics parameters and pixel-dependent contrast thresholds.
- We propose a *receding-horizon update* that performs a few replayed gradient steps per update on a fixed-lag window, alleviating the computational cost compared with offline fitting.

We evaluate the estimator on a synthetic sequence and report ablations that characterize accuracy–latency trade-offs, including recovery of dynamics parameters and the contrast threshold.

Related work: Our work connects three lines of research.

Event-to-tensor pipelines. Many approaches aggregate events into fixed-rate tensors (e.g., voxel grids) and apply standard deep architectures for tasks such as optical flow and video reconstruction [4], [7]. These methods are effective for downstream prediction. However, the aggregation discretizes time and typically does not yield a *normalized likelihood* over the raw event timestamps. As a result, they are not directly suited to maximum-likelihood identification of continuous-time dynamics (and thresholds) from event streams, especially in an online setting where parameters must be adapted from timing information.

Model-based and surrogate-objective methods. Complementary approaches incorporate event-generation mechanisms

for reconstruction and filtering, or optimize surrogate objectives such as contrast maximization and alignment under a motion hypothesis [8], [17]–[19]. However, these methods typically optimize task-specific surrogates (e.g., alignment/contrast) or reconstruction losses rather than a point-process likelihood over event times and marks. Moreover, threshold uncertainty is often handled by calibration or fixed settings [14], [15], whereas we treat the thresholds as learnable parameters that are estimated jointly with the dynamics within a single likelihood-based framework.

Temporal point processes and continuous-time neural dynamics. Neural temporal point-process models such as RMTTP [21] and Neural Hawkes [22] provide flexible likelihoods for marked sequences, while continuous-time neural models such as Neural ODEs and latent/jump variants provide convenient representations of dynamics under irregular observations [20], [23], [24]. A direct application of generic point-process training to event cameras is challenging because the mark space is extremely large (pixel locations and polarities) and the observation model is *per-pixel history dependent* due to the reset at each firing event. Our work exploits this structure explicitly by (i) defining the intensity through a contrast-threshold residual computed from a Neural ODE state via a differentiable state-to-image model, and (ii) making online maximum-likelihood updates practical using a compact per-pixel memory and a fixed-lag receding-horizon scheme with bounded per-update computation.

II. BACKGROUND

A. Neural ODEs for continuous-time dynamics

A Neural Ordinary Differential Equation (Neural ODE) represents latent dynamics in continuous time by learning a vector field. Let $\mathbf{x}(t) \in \mathbb{R}^n$ denote the latent state at continuous time t . A Neural ODE specifies the initial value problem:

$$\frac{d\mathbf{x}(t)}{dt} = f_{\vartheta}(\mathbf{x}(t), t), \quad (1)$$

where f_{ϑ} is parameterized by trainable parameters ϑ (e.g., neural-network weights and/or physical parameters). Given an initial condition $\mathbf{x}(t_0)$, the state at time t satisfies

$$\mathbf{x}(t) = \mathbf{x}(t_0) + \int_{t_0}^t f_{\vartheta}(\mathbf{x}(\tau), \tau) d\tau. \quad (2)$$

We obtain $\mathbf{x}(t)$ numerically with an ODE solver, which we denote by

$$\mathbf{x}(t) = \text{ODESolve}(f_{\vartheta}, \mathbf{x}(t_0), t_0, t).$$

The ODE parameters are learned by minimizing a given task loss

$$\min_{\vartheta} \ell(\vartheta),$$

where ℓ is typically defined from data-fit terms. Training requires gradients of ℓ with respect to ϑ . Backpropagating through the internal steps of an ODE solver can be memory intensive for long time horizons. Neural ODEs are therefore

often trained using the adjoint sensitivity method [20]. This introduces the adjoint state

$$\mathbf{a}(t) = \frac{\partial \ell(\vartheta)}{\partial \mathbf{x}(t)}, \quad (3)$$

which propagates sensitivities backward in time and yields parameter gradients via $\partial f_{\vartheta}/\partial \vartheta$.

B. Event cameras and contrast-threshold events

An event camera outputs an asynchronous stream of per-pixel brightness-change events

$$\mathcal{E} = \{(\mathbf{u}_k, t_k, p_k)\}_{k=1}^K, \quad (4)$$

where $\mathbf{u}_k \in \Omega = \{0, \dots, W_{\text{img}} - 1\} \times \{0, \dots, H_{\text{img}} - 1\}$ is a 2-D pixel location, $t_k \in \mathbb{R}_{\geq 0}$ is a timestamp, and $p_k \in \{+1, -1\}$ is the polarity (sign of the brightness change).

A common generative description is based on *log-intensity* $L(\mathbf{u}, t) = \log(I(\mathbf{u}, t) + \varepsilon)$ (with small $\varepsilon > 0$ for numerical stability) for any pixel location $\mathbf{u} \in \Omega$ and an idealized contrast-threshold mechanism: for each pixel, the sensor integrates the log-intensity change since the most recent event at that pixel and triggers a new event when the accumulated change reaches a threshold. Let $t^-(\mathbf{u}; t)$ be the most recent event time at pixel \mathbf{u} strictly before t . Then, an event with polarity p occurs at the *first* time t after $t^-(\mathbf{u}; t)$ such that

$$L(\mathbf{u}, t) - L(\mathbf{u}, t^-(\mathbf{u}; t)) = pC(\mathbf{u}), \quad (5)$$

where $C(\mathbf{u}) > 0$ is the (possibly pixel-dependent) contrast threshold. Two aspects are important for modeling and learning: **Per-pixel history dependence.** The reference time $t^-(\mathbf{u}; t)$ resets after each event, so the residual that determines the next trigger depends on the last event time at the same pixel. **Unknown thresholds.** Thresholds can vary across pixels and conditions. For example, bias settings, temperature changes, sensor aging, or internal auto-calibration can shift the effective threshold over time. Hence, $C(\mathbf{u})$ is often not precisely known a priori (and may not be provided by the device API).

C. Temporal marked point processes and conditional intensity

A temporal point process models random events occurring at continuous times. A *marked* point process associates a *mark* m to each event time. For event cameras, a natural choice is to treat the mark as the pair

$$m = (\mathbf{u}, p) \in \mathcal{M} = \Omega \times \{+1, -1\},$$

i.e., the mark encodes *which pixel fired* and *with which polarity*. In other words, this can be seen as a $(2W_{\text{img}}H_{\text{img}})$ -dimensional multivariate point process, one dimension per (\mathbf{u}, p) .

Let $\mathcal{E}_{<t}$ denote the event history strictly before time t . The *conditional intensity* $\lambda_m(t | \mathcal{E}_{<t})$ is the instantaneous rate of observing an event with mark m at time t :

$$\lambda_m(t | \mathcal{E}_{<t}) = \lim_{\Delta t \rightarrow 0} \frac{1}{\Delta t} \times \Pr(\text{event with mark } m \text{ in } [t, t + \Delta t) | \mathcal{E}_{<t}).$$

The corresponding total intensity (summing over all marks) is

$$\Lambda(t | \mathcal{E}_{<t}) = \sum_{m \in \mathcal{M}} \lambda_m(t | \mathcal{E}_{<t}).$$

Given an observed event stream $\mathcal{E} = \{(\mathbf{u}_k, t_k, p_k)\}_{k=1}^K$ on $[t_0, T]$, define $m_k = (\mathbf{u}_k, p_k)$. The log-likelihood of a marked point process has the standard form [25]

$$\log p(\mathcal{E}) = \sum_{k=1}^K \log \lambda_{m_k}(t_k | \mathcal{E}_{<t_k}) - \int_{t_0}^T \Lambda(t | \mathcal{E}_{<t}) dt. \quad (6)$$

The integral term is called the *compensator* (also known as the *survival term*). It ensures proper normalization by accounting for the probability that no additional events occur beyond those observed. Intuitively, it uses information from time and mark regions where the stream is silent, and it prevents degenerate solutions in which the likelihood is increased by driving intensities to arbitrarily large values.

This formulation aligns with event-camera data in two ways. First, event cameras produce irregular (or, non periodic) timestamps and discrete marks, and the intensity-based likelihood assigns a density to both time and mark. Second, one can choose $\lambda_m(t | \mathcal{E}_{<t})$ to depend on a *history-dependent residual* that mirrors (5). For example, define

$$r(\mathbf{u}, p, t) = L(\mathbf{u}, t) - L(\mathbf{u}, t^-(\mathbf{u}; t)) - pC(\mathbf{u}),$$

and then apply a smooth positive mapping from r onto $\lambda_{(\mathbf{u}, p)}$ (see Section IV-B). Under this construction, the point-process model can be viewed as a probabilistic relaxation of hard contrast-threshold triggering. It avoids explicit root finding for threshold crossing times while yielding a tractable objective (negative log-likelihood) for gradient-based learning with continuous-time latent dynamics.

III. PROBLEM FORMULATION

Let us consider an event camera observing a moving scene (e.g., a moving object or a moving camera) whose motion is governed by a latent continuous-time state $\mathbf{x}(t) \in \mathbb{R}^n$. The state evolves according to continuous-time dynamics parameterized by unknown parameters ϑ (1). The camera outputs only the resulting asynchronous event stream (4). Event timing depends on changes in log-intensity and on the contrast threshold (5). Here, we treat the threshold as unknown and parameterize it as $C(\mathbf{u}) = C_{\psi}(\mathbf{u})$ for any $\mathbf{u} \in \Omega$ with learnable parameters ψ . Given \mathcal{E} , our goal is to estimate (ϑ, ψ) by maximum likelihood under a marked point-process observation model (6).

To connect the latent state trajectory to the event measurements, we use a differentiable state-to-image model that *predicts* the intensity \hat{L} :

$$\hat{L}(\mathbf{u}, t; \vartheta) = \mathcal{R}(\mathbf{u}, \mathbf{x}(t)), \quad (7)$$

where \mathcal{R} is a renderer (or decoder) that maps the state to the image domain (note that dependence on ϑ is through $\mathbf{x}(t)$). Let $t^-(\mathbf{u}; t)$ denote the most recent event time at pixel $\mathbf{u} \in \Omega$ strictly before time t . We define the history-dependent log-intensity increment relative to $t^-(\mathbf{u}; t)$ as

$$\Delta \hat{L}(\mathbf{u}, t; \vartheta) = \hat{L}(\mathbf{u}, t; \vartheta) - \hat{L}(\mathbf{u}, t^-(\mathbf{u}; t); \vartheta). \quad (8)$$

Under the contrast-threshold rule (5), an event at pixel u with polarity p is triggered when the increment reaches the threshold. Accordingly, we expect the threshold-crossing residual $\Delta\hat{L}(\mathbf{u}, t; \vartheta) - pC_{\psi}(\mathbf{u})$ to be close to zero at event times. In the following section, we construct a history-dependent point-process intensity by mapping this residual to a positive event rate, yielding a differentiable maximum-likelihood objective.

IV. PROPOSED METHOD

A. Overview of the proposed method

Event streams can be long, so we seek per-update computation that does not grow with elapsed time. In our model, the history dependence enters only through the most recent event at the same pixel, so the event likelihood can be evaluated using the per-pixel memory $(t^-(\mathbf{u}), \hat{L}^-(\mathbf{u}))$ defined in the previous section. The compensator term used in the log-likelihood (6) requires summing intensities over the full pixel grid, which we approximate by Monte Carlo subsampling over pixels. We then optimize a fixed-lag receding-horizon objective on a receding horizon window and detach the boundary memory at the window start, yielding bounded backpropagation through the gradients across windows.

B. Likelihood objective

Using (8), let us define the residual

$$\varphi_{\mathbf{u},p}(t; \vartheta, \psi) = \Delta\hat{L}(\mathbf{u}, t; \vartheta) - pC_{\psi}(\mathbf{u}). \quad (9)$$

We model events as samples from a history-dependent marked point process with conditional intensity $\lambda_{\mathbf{u},p}(t | \mathcal{E}_{<t}; \vartheta, \psi)$. We abbreviate $\lambda_{\mathbf{u},p}(t | \mathcal{E}_{<t}; \vartheta, \psi)$ as $\lambda_{\mathbf{u},p}(t)$

$$\lambda_{\mathbf{u},p}(t) = \lambda_{\mathbf{u},p}(t | \mathcal{E}_{<t}; \vartheta, \psi). \quad (10)$$

We use a smooth positive parameterization that increases as the residual approaches the threshold boundary:

$$\lambda_{\mathbf{u},p}(t) = \lambda_0 + \text{softplus}\left(\beta - \gamma |\varphi_{\mathbf{u},p}(t; \vartheta, \psi)|\right), \quad (11)$$

where $\text{softplus}(s) = \log(1 + \exp(s))$ is the softplus function (a smooth approximation of $\max\{0, s\}$), $\lambda_0 \geq 0$ is a floor rate, $\beta \in \mathbb{R}$ sets the peak level, and $\gamma > 0$ controls sharpness. Defining the distance-to-threshold $d = |\varphi_{\mathbf{u},p}(t; \vartheta, \psi)|$, (11) is a decreasing function of d with peak value $\lambda_0 + \text{softplus}(\beta)$ at $d = 0$. Fig. 2 illustrates how γ controls the concentration of probability mass near $d \approx 0$. For large γ (and small λ_0), events concentrate near $|\varphi_{\mathbf{u},p}(t; \vartheta, \psi)| \approx 0$, providing a differentiable surrogate of contrast-threshold triggering. In this paper, we use (11) as a practical likelihood model, and learn (ϑ, ψ) and treat $(\lambda_0, \beta, \gamma)$ as fixed hyperparameters.

Let T be the final observation time and define the total intensity $\Lambda(t) = \sum_{\mathbf{u} \in \Omega} \sum_{p \in \{+1, -1\}} \lambda_{\mathbf{u},p}(t)$. Under a marked temporal point process, the probability density of observing the marked event stream \mathcal{E} on $[t_0, T]$ can be written as

$$p(\mathcal{E} | \vartheta, \psi) = \prod_{k=1}^K \lambda_{\mathbf{u}_k, p_k}(t_k) \exp\left(-\int_{t_0}^T \Lambda(t) dt\right), \quad (12)$$

$$\Lambda(t) = \sum_{\mathbf{u} \in \Omega} \sum_{p \in \{+1, -1\}} \lambda_{\mathbf{u},p}(t).$$

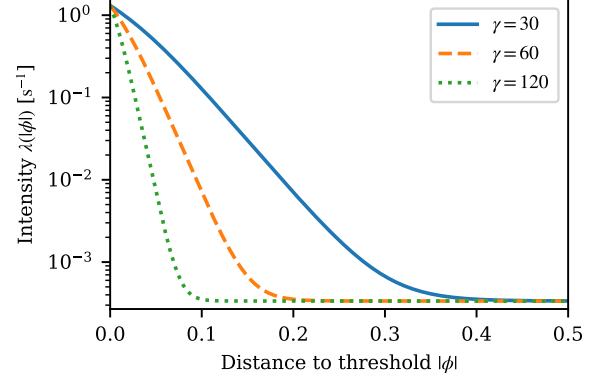


Fig. 2: Surrogate intensity (11) as a function of the distance-to-threshold $d = |\varphi|$. Increasing γ concentrates events closer to $d = 0$ (here shown for $\gamma \in \{30, 60, 120\}$; log-scale on the y -axis).

Taking the logarithm yields

$$\log p(\mathcal{E} | \vartheta, \psi) = \sum_{k=1}^K \log \lambda_{\mathbf{u}_k, p_k}(t_k) - \int_{t_0}^T \Lambda(t) dt. \quad (13)$$

Then, we minimize $\ell(\vartheta, \psi) = -\log p(\mathcal{E} | \vartheta, \psi)$. The exponential factor in (12) is often called a *compensator* (or, survival) term: it is the probability of generating *no additional events* beyond those observed, so that it utilizes information for regions where the stream is silent.

1) *Monte Carlo approximation and augmented dynamics:* Summing over all pixels (and both polarities) at every time is expensive, as it requires evaluating $\lambda_{\mathbf{u},p}(t)$ over the full $2|\Omega|$ mark space repeatedly for high-resolution sensors. We approximate the pixel sum by Monte Carlo sampling:

$$\sum_{\mathbf{u} \in \Omega} \sum_p \lambda_{\mathbf{u},p}(t) \approx \frac{|\Omega|}{S} \sum_{s=1}^S \sum_{p \in \{+1, -1\}} \lambda_{\tilde{\mathbf{u}}_s, p}(t), \quad (14)$$

where $\tilde{\mathbf{u}}_s$ are pixels sampled uniformly from Ω and S is the number of sampled pixels. A standard implementation augments the ODE with an auxiliary state $z(t)$ to accumulate the survival integral:

$$\frac{d}{dt} \begin{bmatrix} \mathbf{x}(t) \\ z(t) \end{bmatrix} = \begin{bmatrix} f_{\vartheta}(\mathbf{x}(t), t) \\ \sum_{\mathbf{u}, p} \lambda_{\mathbf{u},p}(t) \end{bmatrix}. \quad (15)$$

Integrating (15) yields the compensator term in the marked point-process log-likelihood, which can be used for the forward update:

$$z(T) - z(t_0) = \int_{t_0}^T \Lambda(t) dt. \quad (16)$$

C. Receding-horizon estimation

Let $t_0 = \tau_0 < \tau_1 < \dots < \tau_M = T$ be the parameter-update times. In this paper, for simplicity, this streaming schedule is given by the update period Δt_{upd} , i.e., $\tau_m = \tau_0 + m \Delta t_{\text{upd}}$. Rather than repeatedly optimizing over the growing prefix $\mathcal{E}_{\leq \tau_m}$, we update parameters on a *moving time window*.

Introduce a horizon length $\Delta > 0$ and define the window event set

$$\mathcal{E}_{(\tau_m - \Delta, \tau_m]} = \{(\mathbf{u}_k, t_k, p_k) \in \mathcal{E} \mid \tau_m - \Delta < t_k \leq \tau_m\}. \quad (17)$$

1) *Windowed negative log-likelihood with detached boundary memory*: We utilize the event history up to the window start by a *boundary memory*, which we denote by $s_{\tau_m - \Delta}$. To be specific, for each pixel $\mathbf{u} \in \Omega$, define the boundary last-event time

$$t_{\tau_m - \Delta}^-(\mathbf{u}) = \max_{k: \mathbf{u}_k = \mathbf{u}, t_k \leq \tau_m - \Delta} t_k, \quad (18)$$

Then, we collect these two per-pixel quantities as

$$s_{\tau_m - \Delta} = \left\{ (t_{\tau_m - \Delta}^-(\mathbf{u}), \hat{L}_{\tau_m - \Delta}^-(\mathbf{u})) \right\}_{\mathbf{u} \in \Omega}.$$

Conditioned on this memory, the point-process likelihood over the window has the same form as (12)–(13), but restricted to the interval $[\tau_m - \Delta, \tau_m]$. We define the windowed objective

$$\begin{aligned} \ell_m^{\text{win}}(\vartheta, \psi) = & - \sum_{(\mathbf{u}_k, t_k, p_k) \in \mathcal{E}_{(\tau_m - \Delta, \tau_m]}} \log \lambda_{\mathbf{u}_k, p_k}(t_k) \\ & + \int_{\tau_m - \Delta}^{\tau_m} \Lambda(t) dt. \end{aligned} \quad (19)$$

To evaluate (19), we initialize the memory at $\tau_m - \Delta$ with $s_{\tau_m - \Delta}$, replay events in $\mathcal{E}_{(\tau_m - \Delta, \tau_m]}$ in chronological order to compute the event term, and approximate the compensator integral using the Monte Carlo approximation (14). To keep the computation graph bounded, we *detach* gradients through $s_{\tau_m - \Delta}$, so backpropagation is restricted to the current window. At each update time τ_m , we take a small number of gradient steps on (19), which plays a similar role to a few iterations in moving-horizon estimators.

D. Training and adjoint gradients for event likelihoods

Recall that our online updates minimize the windowed negative log-likelihood (19); the objective consists of a sum over discrete event times and a continuous-time compensator. Since it exhibits continuous-time and discrete terms, the adjoint evolves continuously between events and receives jump updates at event times.

For update m , let us denote the window interval for the notational simplicity $[t_a, t_b] = [\tau_m - \Delta, \tau_m]$ and condition on the detached boundary memory $s_{\tau_m - \Delta}$ at t_a (Section IV-C). We define the adjoint

$$\mathbf{a}(t) = \frac{\partial \ell_m^{\text{win}}(\vartheta, \psi)}{\partial \mathbf{x}(t)}, \quad t \in [t_a, t_b].$$

Between event times, $\mathbf{x}(t)$ follows $\dot{\mathbf{x}}(t) = f_\vartheta(\mathbf{x}(t), t)$ and the adjoint satisfies

$$\frac{d\mathbf{a}(t)}{dt} = - \left(\frac{\partial f_\vartheta(\mathbf{x}(t), t)}{\partial \mathbf{x}} \right)^\top \mathbf{a}(t) - \frac{\partial \Lambda(t)}{\partial \mathbf{x}}, \quad (20)$$

where $\Lambda(t) = \sum_{\mathbf{u} \in \Omega} \sum_{p \in \{+1, -1\}} \lambda_{\mathbf{u}, p}(t)$ is the total intensity (approximated by the Monte Carlo estimator (14) in practice). By the chain rule,

$$\frac{\partial \Lambda(t)}{\partial \mathbf{x}} = \sum_{\mathbf{u} \in \Omega} \sum_{p \in \{+1, -1\}} \frac{\partial \lambda_{\mathbf{u}, p}(t)}{\partial \varphi_{\mathbf{u}, p}(t)} \frac{\partial \varphi_{\mathbf{u}, p}(t)}{\partial \mathbf{x}}, \quad (21)$$

$$\frac{\partial \lambda_{\mathbf{u}, p}(t)}{\partial \varphi_{\mathbf{u}, p}(t)} = -\gamma \sigma(\beta - \gamma |\varphi_{\mathbf{u}, p}(t)|) \text{sign}(\varphi_{\mathbf{u}, p}(t)), \quad (22)$$

where $\sigma(\cdot)$ is the logistic sigmoid (since $d \text{softplus}(z)/dz = \sigma(z)$). Conditioned on the per-pixel memory $(t^-(\mathbf{u}), \hat{L}^-(\mathbf{u}))$ within the window, $\varphi_{\mathbf{u}, p}(t) = \hat{L}(\mathbf{u}, t; \vartheta) - \hat{L}^-(\mathbf{u}) - p C_\psi(\mathbf{u})$, hence $\partial \varphi_{\mathbf{u}, p}(t)/\partial \mathbf{x} = \partial \hat{L}(\mathbf{u}, t; \vartheta)/\partial \mathbf{x} = \partial \mathcal{R}(\mathbf{u}, \mathbf{x}(t), t)/\partial \mathbf{x}$ (recall that \mathcal{R} is defined in (7)). When using the Monte Carlo estimator (14), we simply differentiate through the sampled sum.

For each event time $(\mathbf{u}_k, t_k, p_k) \in \mathcal{E}_{(\tau_m - \Delta, \tau_m]}$, the loss receives the discrete contribution $-\log \lambda_{\mathbf{u}_k, p_k}(t_k)$, which induces an adjoint jump

$$\mathbf{a}(t_k^-) = \mathbf{a}(t_k^+) - \frac{\partial}{\partial \mathbf{x}} \log \lambda_{\mathbf{u}_k, p_k}(t_k). \quad (23)$$

For the point-process event term, the jump in (23) uses

$$\frac{\partial}{\partial \mathbf{x}} \log \lambda_{\mathbf{u}_k, p_k}(t_k) = \frac{1}{\lambda_{\mathbf{u}_k, p_k}(t_k)} \frac{\partial \lambda_{\mathbf{u}_k, p_k}(t_k)}{\partial \varphi} \frac{\partial \varphi_{\mathbf{u}_k, p_k}(t_k)}{\partial \mathbf{x}},$$

with $\partial \lambda/\partial \varphi$ given in (22) and $\partial \varphi/\partial \mathbf{x} = \partial \hat{L}(\mathbf{u}_k, t_k; \vartheta)/\partial \mathbf{x}$ as above.

The gradient with respect to dynamics parameters is accumulated as

$$\frac{d\ell_m^{\text{win}}}{d\vartheta} = \int_{\tau_m - \Delta}^{\tau_m} \mathbf{a}(t)^\top \frac{\partial f_\vartheta(\mathbf{x}(t), t)}{\partial \vartheta} dt, \quad (24)$$

and the gradient with respect to ψ is

$$\begin{aligned} \frac{\partial \ell_m^{\text{win}}}{\partial \psi} = & - \sum_{(\mathbf{u}_k, t_k, p_k) \in \mathcal{E}_{(\tau_m - \Delta, \tau_m]}} \frac{\partial}{\partial \psi} \log \lambda_{\mathbf{u}_k, p_k}(t_k) \\ & + \int_{\tau_m - \Delta}^{\tau_m} \frac{\partial \Lambda(t)}{\partial \psi} dt. \end{aligned} \quad (25)$$

Note that ψ enters the likelihood only through the observation model (via $C_\psi(\mathbf{u})$ inside $\lambda_{\mathbf{u}, p}(t)$), hence $\mathbf{x}(t)$ is independent of ψ (i.e., $\partial \mathbf{x}(t)/\partial \psi = 0$).

E. Algorithm summary

We summarize the receding-horizon estimator that turns a continuous event stream into a sequence of parameter updates. As previously stated, the update schedule is $\tau_m = \tau_0 + m \Delta t_{\text{upd}}$ and the number of replay steps per update is denoted as N_{step} . The horizon length Δ specifies the time window optimized at each update. At each update time τ_m , we form the window event set $\mathcal{E}_{(\tau_m - \Delta, \tau_m]}$ and update the parameters (ϑ, ψ) by minimizing the windowed objective (19) using N_{step} Adam steps, replaying only events in the current window. The per-pixel memory at the window boundary is carried between the updates and detaches the computation graph, which bounds backpropagation depth. Algorithm 1 summarizes the above procedure.

F. Computational cost and memory

For a horizon of duration Δ , let $K_m^{\text{win}} = |\mathcal{E}_{(\tau_m - \Delta, \tau_m]}|$ be the number of events in the current window. One evaluation of the windowed objective (19) costs $\mathcal{O}(K_m^{\text{win}})$ for the event term plus $\mathcal{O}(S)$ intensity evaluations for the Monte Carlo compensator approximation (14). With N_{step} replay steps per update, the per-update cost scales as

$$\mathcal{O}(N_{\text{step}}(K_m^{\text{win}} + S)), \quad (26)$$

Algorithm 1 Receding-horizon event-based parameter estimation (windowed MLE)

Require: Event stream $\mathcal{E} = \{(\mathbf{u}_k, t_k, p_k)\}_{k=1}^K$; update times $\{\tau_m\}_{m=0}^M$ (or, the update period Δt_{upd}); horizon length Δ ; replay steps per update N_{step} ; models f_ϑ and $\hat{L}(\cdot)$; intensity (11); MC pixels S ; step size η .

Ensure: Parameter estimates $\{(\vartheta_m, \psi_m)\}_{m=0}^M$.

- 1: Initialize (ϑ_0, ψ_0) and $\mathbf{x}(\tau_0)$; set $(\vartheta, \psi) \leftarrow (\vartheta_0, \psi_0)$.
 - 2: Initialize stored per-pixel memory s_0 : $\forall \mathbf{u} \in \Omega$, set $t^-(\mathbf{u}) \leftarrow \tau_0$, $\hat{L}^-(\mathbf{u}) \leftarrow \hat{L}(\mathbf{u}, \tau_0; \vartheta)$.
 - 3: **for** $m = 1$ to M **do**
 - 4: Form window events $\mathcal{E}_{(\tau_{m-\Delta}, \tau_m)}$.
 - 5: **for** $e = 1$ to N_{step} **do**
 - 6: Evaluate window loss ℓ_m^{win} (19) using $s_{\tau_m - \Delta}$ as the initial (detached) memory.
Approximate the compensator on $[\tau_m - \Delta, \tau_m]$ by MC pixel subsampling (14).
 - 7: Update parameters $(\vartheta, \psi) \leftarrow (\vartheta, \psi) - \eta \nabla \ell_m^{\text{win}}$.
 - 8: **end for**
 - 9: Update the memory s_m by processing events in $\mathcal{E}_{(\tau_{m-\Delta}, \tau_m)}$: for each $(u_k, t_k, p_k) \in \mathcal{E}_{(\tau_{m-\Delta}, \tau_m)}$, set $t^-(u_k) \leftarrow t_k$ and $\hat{L}^-(u_k) \leftarrow \hat{L}(u_k, t_k; \vartheta)$.
 - 10: Store $(\vartheta_m, \psi_m) \leftarrow (\vartheta, \psi)$.
 - 11: **end for**
-

which is bounded when Δ is fixed. Memory usage is dominated by the per-pixel memory $\mathcal{O}(|\Omega|)$ and storing the current window events $\mathcal{O}(K_m^{\text{win}})$.

V. NUMERICAL EXPERIMENTS

We evaluate the proposed receding-horizon maximum-likelihood estimator on a synthetic event-camera sequence. All experiments are implemented in Python/PyTorch and executed on Google Colab (with a CUDA-enabled GPU runtime). Key parameters and hyperparameters are summarized in Table I.

A. Problem setting

We render a moving Gaussian blob on an image grid of size $H = W = 64$ and generate events by the ideal contrast-threshold rule (5). The goal is to estimate the continuous-time dynamics parameters and a pixel-dependent contrast threshold map from the event stream.

1) *Latent center and dynamics:* Let $\mathbf{c}(t) \in \mathbb{R}^2$ denote the blob center given by

$$\mathbf{c}(t) = \mathbf{c}_0(t) + \mathbf{z}(t), \quad \mathbf{z}(t) = [x(t), y(t)]^\top, \quad (27)$$

where $\mathbf{c}_0(t)$ is a known base-center drift and is given by

$$\mathbf{c}_0(t) = \mathbf{c}_{\text{base}} + \begin{bmatrix} A \sin(2\pi t/T_1) \\ B \sin(2\pi t/T_2) \end{bmatrix}, \quad (28)$$

where $\mathbf{c}_{\text{base}} = (32, 32)$ and $A = B = 22, T_1 = 1, T_2 = 1.3$ are given constants. The offset state $\mathbf{z}(t)$ follows the stable-focus ODE

$$\dot{x}(t) = -\alpha x(t) - \omega y(t), \quad (29)$$

$$\dot{y}(t) = \omega x(t) - \alpha y(t), \quad (30)$$

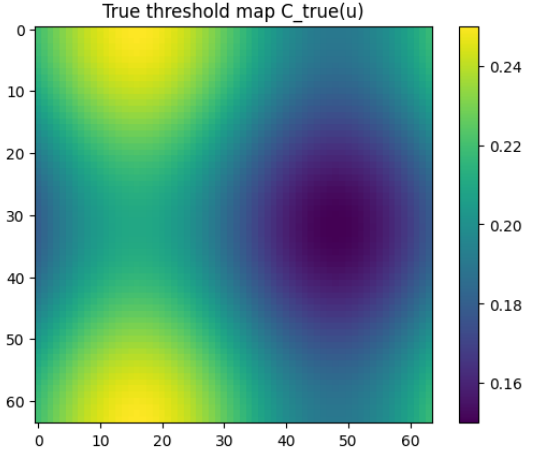


Fig. 3: True pixel dependent threshold map $C(\cdot)$.

with initial condition $[x(0), y(0)] = [12.0, 0.0]$. In our synthetic data, events are generated using $(\alpha, \omega) = (0.265, 7.52)$.

2) *State-to-image observation model:* Given $\mathbf{c}(t)$, the rendered intensity is given by the Gaussian-blob model:

$$I(\mathbf{u}, t) = I_{\text{bg}} + I_{\text{amp}} \exp\left(-\frac{\|\mathbf{u} - \mathbf{c}(t)\|^2}{2\sigma^2}\right), \quad (31)$$

with fixed $(I_{\text{bg}}, I_{\text{amp}}, \sigma)$ (Table I), where $\mathbf{u} = (u_x, u_y) \in \Omega$ is a pixel location (in pixel units), consistent with the event-stream notation in Section II-B. The parameters I_{bg} and I_{amp} set the background level and the contrast (amplitude) of the rendered blob. We do not estimate them from events: event generation depends on *log-intensity increments* $\Delta L(\mathbf{u}, t)$, so additive offsets in L do not change events, and the overall brightness scale is weakly identifiable and strongly coupled to the unknown contrast threshold. Fixing $(I_{\text{bg}}, I_{\text{amp}})$ removes this ambiguity and isolates dynamics and threshold estimation. The parameter σ is the spatial standard deviation of the Gaussian blob (in pixels) and thus controls the apparent object size; larger σ activates more pixels and increases event density, while smaller σ produces sparser events. We define the log-intensity used for event synthesis as

$$\hat{L}(\mathbf{u}, t; \vartheta) = \mathcal{R}(\mathbf{u}, \mathbf{c}(t)) = \log(I(\mathbf{u}, t) + \epsilon) \quad (32)$$

where the small parameter $\epsilon = 10^{-3}$ is added for numerical stability.

3) *Event synthesis and pixel-dependent threshold:* We render intensity frames at $\text{fps} = 120$ and generate events by threshold crossings of (5). The sequence duration is $T = 13s$. We consider a pixel-dependent threshold field

$$C(\mathbf{u}) = C_{\text{base}} + 0.03 \sin\left(2\pi \frac{u_x}{W_{\text{img}}}\right) + 0.02 \cos\left(2\pi \frac{u_y}{H_{\text{img}}}\right), \quad (33)$$

with $C_{\text{base}} = 0.2$, where u_x and u_y represents respectively the x and the y of the pixel location \mathbf{u} . Fig. 6 shows the true threshold map $C(\mathbf{u})$ and Fig. 4 shows representative frame and event snapshots.

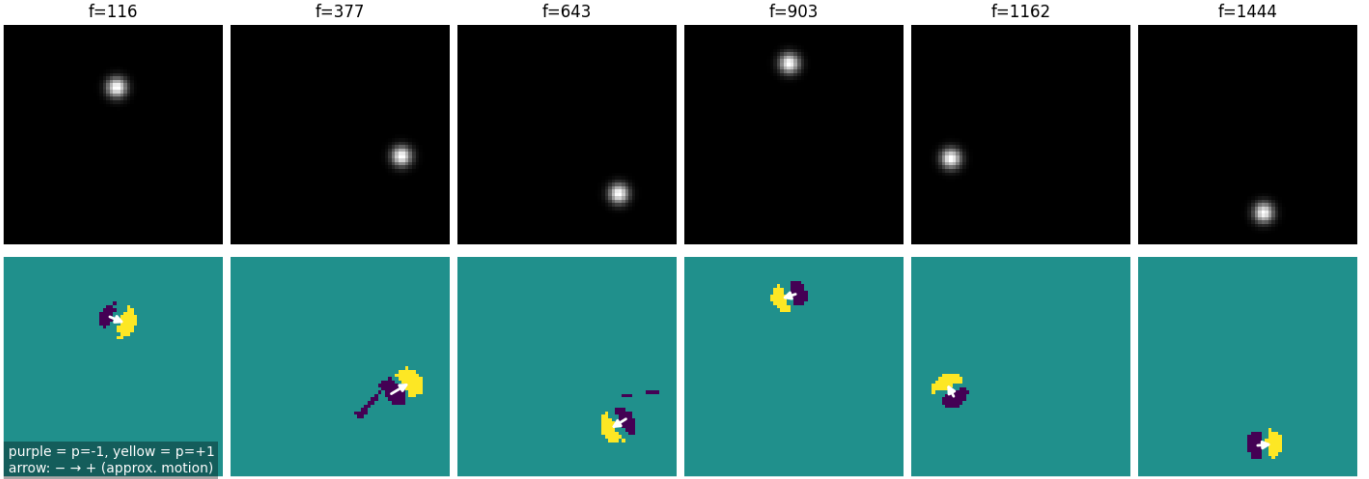


Fig. 4: Representative snapshots from the synthetic event-camera sequence. Top: rendered intensity frames. Bottom: corresponding event images in polarity mode (yellow: $p = +1$, purple: $p = -1$, white arrow: approximated motion).

B. Estimation task

For the dynamics parameters, we aim to estimate

$$\vartheta = \{\alpha, \omega\}. \quad (34)$$

Directly learning all the thresholds within Ω requires $H_{\text{img}}W_{\text{img}}$ parameters ($H_{\text{img}} = W_{\text{img}} = 64$, hence $H_{\text{img}}W_{\text{img}} = 4096$) and is poorly conditioned in regions with few/no events. Thus, we use a low-dimensional parameterization:

$$\psi = \{C_{\text{base}}, \eta\}, \quad C_{\psi}(\mathbf{u}) = C_{\text{base}} + \delta_{\eta}(\mathbf{u}), \quad (35)$$

where C_{base} is a global offset and $\eta \in \mathbb{R}^{H_{\text{img}}^c \times W_{\text{img}}^c}$ is a learnable coarse-grid field with $H_{\text{img}}^c \times W_{\text{img}}^c = 8 \times 8$. Then, for each pixel $\mathbf{u} \in \Omega$, the residual $\delta_{\eta}(\mathbf{u})$ is obtained by converting the coarse-grid field $\eta \in \mathbb{R}^{H_{\text{img}}^c \times W_{\text{img}}^c}$ to a full-resolution map on the $H_{\text{img}} \times W_{\text{img}}$ pixel grid via bilinear interpolation. Concretely, $\delta_{\eta}(\mathbf{u})$ is computed as a convex combination (weighted average) of the four coarse-grid values surrounding the location of \mathbf{u} , with nonnegative weights that sum to one. With this choice, the number of unknown thresholds is $1 + H_{\text{img}}^c W_{\text{img}}^c = 65$ (one scalar C_{base} plus 8×8 coefficients). The compensator integral is approximated by the Monte Carlo pixel subsampling with $S = 512$. We perform receding-horizon updates every $\Delta t_{\text{upd}} = 0.4\text{s}$ and run $N_{\text{step}} = 30$ replayed Adam steps per update on the current window.

C. Simulation results

1) Learning curves with a fixed horizon ($H = 15$):

We report simulation results on the synthetic dataset in Section V-A. We fix the horizon length to $H = 15$ (window length $\Delta = H \Delta t_{\text{upd}}$) and record parameter estimates after each online update.

Fig. 5 shows the learning curves of the dynamics parameters $(\hat{\alpha}, \hat{\omega})$. Both estimates exhibit a transient phase in early episodes and then converge close to the ground truth after a moderate number of updates; after convergence, the estimates

TABLE I: Estimated parameters and key hyperparameters in the numerical experiments (pixel-dependent threshold only).

Item	Value / description
<i>Renderer / data (fixed)</i>	
Grid size ($H_{\text{img}}, W_{\text{img}}$)	64×64
Base center	$c_{\text{base}} = (32, 32)$
Drift parameters	$A = B = 22 \text{ px}, T_1 = 1.0\text{s}, T_2 = 1.3\text{s}$
Intensity params	$(I_{\text{bg}}, I_{\text{amp}}, \sigma) = (0.15, 0.75, 2.0)$
Log eps (data / model)	$\epsilon = 10^{-3}$
Frame rate & duration	$\text{fps} = 120, T = 13.0\text{s}$
<i>Ground truth (synthetic)</i>	
Dynamics (used to generate data)	$(\alpha, \omega) = (0.265, 7.52)$
True threshold field	Eq. (33)
<i>Unknown parameters to be estimated</i>	
Dynamics	$\vartheta = \{\alpha, \omega\}$
Threshold parameters	$\psi = \{C_{\text{base}}, \eta\}$ in Eq. (35)
<i>Likelihood approximation</i>	
Update cadence; replay steps	$\Delta t_{\text{upd}} = 0.4\text{s}; N_{\text{step}} = 30$
MC pixels	$S = 512$
Fixed-lag horizon	$\Delta = H \Delta t_{\text{upd}}$

remain stable over subsequent episodes. Fig. 3 compares the estimated pixel-dependent threshold map $\hat{C}(\mathbf{u})$ with the ground truth $C(\mathbf{u})$. The estimator recovers the overall spatial structure of $C(\mathbf{u})$, while residual discrepancies are present in regions where fewer events are generated (i.e., pixels that are weakly fired by the motion). This behavior is consistent with the fact that the threshold parameters are effectively constrained only through pixels that become active during the sequence.

2) *Horizon ablation* ($H = 1, \dots, 19$): We next study the effect of the horizon length by sweeping $H \in \{1, \dots, 19\}$ while keeping all other settings fixed. We evaluate the final

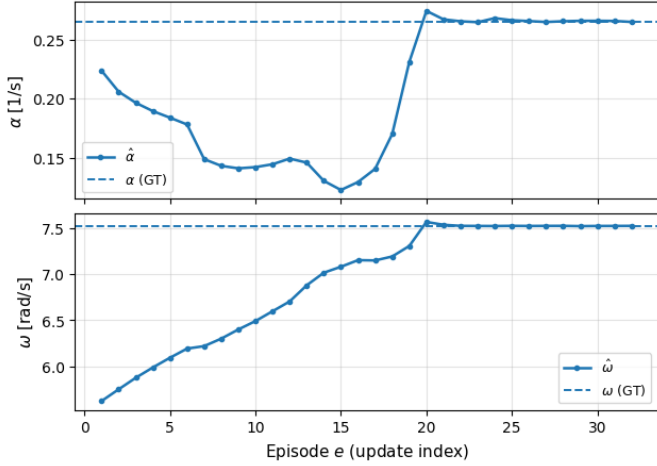


Fig. 5: Learning curves for a fixed horizon $H = 15$. **Top:** $\hat{\alpha}$ versus episode e . **Bottom:** $\hat{\omega}$ versus episode e . Dashed lines indicate the ground truth.

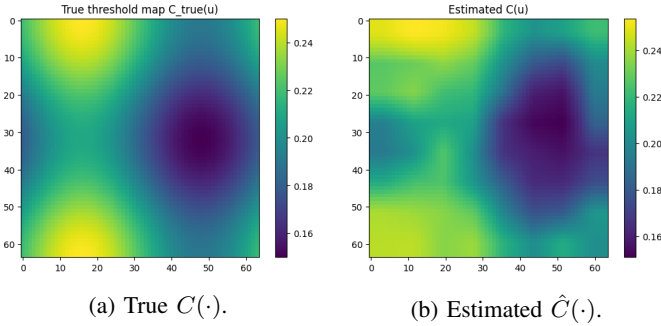


Fig. 6: Estimated Pixel-dependent threshold maps: true $C(\cdot)$ (left) and estimated $\hat{C}(\cdot)$ (right).

estimation accuracy at the end of the sequence using:

$$\text{RMSE}_\alpha(H) = |\hat{\alpha}(H) - \alpha|, \quad (36)$$

$$\text{RMSE}_\omega(H) = |\hat{\omega}(H) - \omega|, \quad (37)$$

$$\text{RMSE}_C(H) = \sqrt{\frac{1}{|\mathcal{A}|} \sum_{\mathbf{u} \in \mathcal{A}} (\hat{C}_H(\mathbf{u}) - C(\mathbf{u}))^2}, \quad (38)$$

where $\mathcal{A} \subseteq \Omega$ denotes the set of *active* pixels (pixels that emitted at least one event in the sequence), so that the threshold error is not dominated by unobserved regions.

Figs. 7 and 8 report the RMSE values as functions of H . The estimation of ω is particularly sensitive: its error remains large for short horizons ($H \leq 13$), but drops by orders of magnitude once the horizon becomes sufficiently long ($H \geq 14$). The RMSE of α shows a similar improvement in the long-horizon regime. The threshold-map error RMSE_C in Fig. 8 is comparatively similar across H (i.e., RMSE with the order of 10^{-2}), but becomes slightly smaller for larger horizons, reaching its minimum around $H \approx 18$. Fig. 9 shows the computational cost as a function of H ; the mean update time increases gradually with H , although we note that it is still smaller than the update time interval (i.e., $0.4s = 400\text{ms}$).

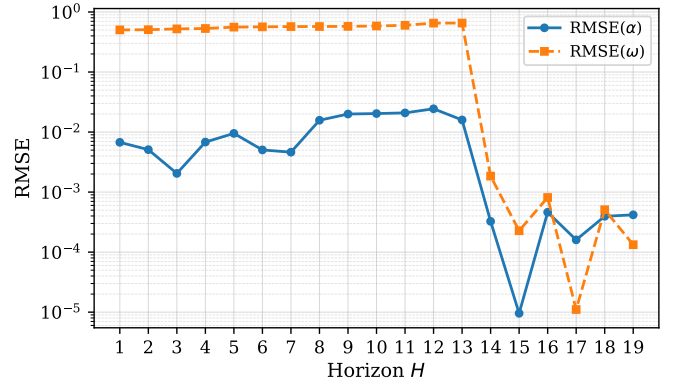


Fig. 7: Horizon ablation. $\text{RMSE}_\alpha(H)$ and $\text{RMSE}_\omega(H)$ as functions of the fixed-lag horizon H (log-scale y-axis).

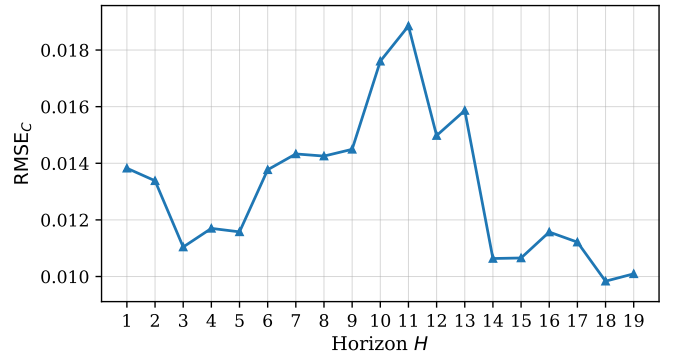


Fig. 8: Horizon ablation. Threshold-map error $\text{RMSE}_C(H)$ over active pixels (38) as a function of H . Note that the y-axis is shown in linear scale for readability.

VI. CONCLUSION AND FUTURE WORK

We presented a likelihood-based estimator for continuous-time dynamics from event-camera streams by combining a Neural ODE state model with a history-dependent marked point-process observation model. The event generation is modeled via a differentiable surrogate of contrast-threshold triggering, and the (pixel-dependent) contrast threshold is treated as an unknown parameter to be estimated jointly with the dynamics. To enable streaming maximum-likelihood training, we approximate the compensator term using Monte Carlo pixel subsampling, and summarize the required per-pixel history with a compact boundary memory (two scalars per pixel). A fixed-lag receding-horizon update then bounds per-update computation by restricting optimization to a sliding time window.

VII. ACKNOWLEDGEMENTS

This work was supported by JST, CRONOS, Japan Grant Number JPMJCS25K3.

REFERENCES

- [1] G. Gallego *et al.*, “Event-based vision: A survey,” *IEEE Transactions on Pattern Analysis and Machine Intelligence*, 2022.

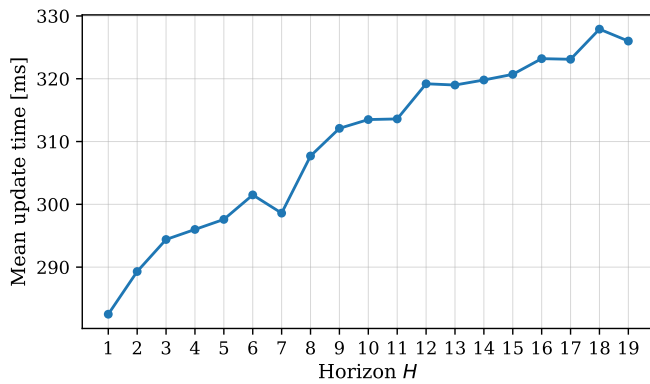


Fig. 9: Mean update time per step as a function of H .

- [2] P. Lichtsteiner, C. Posch, and T. Delbruck, "A 128×128 120 db $15 \mu\text{s}$ latency asynchronous temporal contrast vision sensor," *IEEE Journal of Solid-State Circuits*, vol. 43, no. 2, pp. 566–576, 2008.
- [3] C. Brandli, R. Berner, M.-H. Yang, S.-C. Liu, and T. Delbruck, "A 240×180 130 db $3 \mu\text{s}$ latency global shutter spatiotemporal vision sensor," *IEEE Journal of Solid-State Circuits*, vol. 49, no. 10, pp. 2333–2341, 2014.
- [4] A. Z. Zhu, L. Yuan, K. Chaney, and K. Daniilidis, "Ev-flownet: Self-supervised optical flow estimation for event-based cameras," in *Robotics: Science and Systems (RSS)*, 2018.
- [5] M. Gehrig, M. Millhausler, D. Gehrig, and D. Scaramuzza, "E-RAFT: Dense optical flow from event cameras," in *International Conference on 3D Vision (3DV)*. IEEE, 2021, pp. 197–206.
- [6] M. Gehrig, M. Muglikar, and D. Scaramuzza, "Dense continuous-time optical flow from event cameras," *IEEE Transactions on Pattern Analysis and Machine Intelligence*, vol. 46, no. 7, pp. 4736–4746, 2024.
- [7] H. Rebecq, R. Ranftl, V. Koltun, and D. Scaramuzza, "Events-to-video: Bringing modern computer vision to event cameras," in *Proc. IEEE/CVF CVPR*, 2019.
- [8] C. Scheerlinck, N. Barnes, and R. Mahony, "Continuous-time intensity estimation using event cameras," in *Asian Conference on Computer Vision (ACCV)*, 2018, pp. 308–324.
- [9] L. Pan, R. Hartley, C. Scheerlinck, M. Liu, X. Yu, and Y. Dai, "High frame rate video reconstruction based on an event camera," *IEEE Transactions on Pattern Analysis and Machine Intelligence*, vol. 44, no. 5, pp. 2519–2533, 2022.
- [10] S. Tulyakov, D. Gehrig, S. Georgoulis, J. Erbach, M. Gehrig, Y. Li, and D. Scaramuzza, "Time lens: Event-based video frame interpolation," in *Proc. IEEE/CVF CVPR*, 2021, pp. 16 155–16 164.
- [11] E. Mueggler, H. Rebecq, G. Gallego, T. Delbruck, and D. Scaramuzza, "The event-camera dataset and simulator: Event-based data for pose estimation, visual odometry, and slam," *The International Journal of Robotics Research*, vol. 36, no. 2, pp. 142–149, 2017.
- [12] H. Rebecq, D. Gehrig, and D. Scaramuzza, "Esim: an open event camera simulator," in *Conference on Robot Learning (CoRL)*, 2018.
- [13] D. Gehrig and D. Scaramuzza, "Low-latency automotive vision with event cameras," *Nature*, vol. 629, no. 8014, pp. 1034–1040, 2024.
- [14] T. Stoffregen, C. Scheerlinck, D. Scaramuzza, T. Drummond, N. Barnes, L. Kleeman, and R. Mahony, "Reducing the sim-to-real gap for event cameras," in *European Conference on Computer Vision (ECCV)*, 2020.
- [15] Z. Wang, Y.-S. Ng, P. van Goor, and R. Mahony, "Event camera calibration of per-pixel biased contrast threshold," arXiv:2012.09378, 2020.
- [16] N. Zubic, M. Gehrig, and D. Scaramuzza, "State space models for event cameras," in *Proc. IEEE/CVF CVPR*, 2024, pp. 5819–5828.
- [17] G. Gallego, H. Rebecq, and D. Scaramuzza, "A unifying contrast maximization framework for event cameras, with applications to motion, depth, and optical flow estimation," in *Proc. IEEE CVPR*, 2018.
- [18] T. Stoffregen and L. Kleeman, "Event cameras, contrast maximization and reward functions: an analysis," in *Proc. IEEE/CVF CVPR*, 2019.
- [19] C. Gu, E. Learned-Miller, D. Sheldon, G. Gallego, and P. Bideau, "The spatio-temporal poisson point process: A simple model for the alignment of event camera data," in *Proc. IEEE/CVF ICCV*, 2021.
- [20] R. T. Q. Chen, Y. Rubanova, J. Bettencourt, and D. Duvenaud, "Neural

ordinary differential equations," in *Advances in Neural Information Processing Systems*, 2018.

- [21] N. Du, H. Dai, R. Trivedi, U. Upadhyay, M. Gomez-Rodriguez, and L. Song, "Recurrent marked temporal point processes: Embedding event history to vector," in *Proc. ACM SIGKDD (KDD)*, 2016, pp. 1555–1564.
- [22] H. Mei and J. M. Eisner, "The neural hawkes process: A neurally self-modulating multivariate point process," in *Advances in Neural Information Processing Systems*, 2017.
- [23] Y. Rubanova, R. T. Q. Chen, and D. Duvenaud, "Latent ordinary differential equations for irregularly-sampled time series," in *Advances in Neural Information Processing Systems*, 2019.
- [24] C. Herrera, F. Krach, and J. Teichmann, "Neural jump ordinary differential equations: Consistent continuous-time prediction and filtering," in *International Conference on Learning Representations (ICLR)*, 2021.
- [25] D. J. Daley and D. Vere-Jones, *An Introduction to the Theory of Point Processes*, 2nd ed. Springer, 2007.